Supporting Information

Aromatic ionene topology and counterion-tuned gelation of acidic aqueous solutions

Jürgen Bachl,[a] *Oscar Bertran,*[b] *Judith Mayr,*[a] *Carlos Alemán**[,c,d] *and David Díaz Díaz**[,a,e]

[a] Institut für Organische Chemie, Universität Regensburg, Universitätsstr. 31, 93053 Regensburg, Germany. [b] Departament de Física Aplicada, EEI, Universitat Politècnica de Catalunya, Av. Pla de la Massa, 8, 08700 Igualada, Spain. [c] Departament d'Enginyeria Química, EEBE, Universitat Politècnica de Catalunya, C/ Eduard Maristany, 10-14, 08019, Barcelona, Spain. [d] Barcelona Research Center for Multiscale Science and Engineering, Universitat Politècnica de Catalunya
C/ Eduard Maristany, 10-14, 08019, Barcelona, Spain. [e] IQAC-CSIC, Jordi Girona 18-26, 08034 Barcelona, Spain.

List of Contents

1. Synthesis of ionenes

1,2-, 1,3- and 1,4-ionene polymers containing DABCO and *N*,*N'*-(*x*-phenylene)dibenzamide (*x* = *ortho-*/*meta-*/*para-*, respectively) linkages were synthesized via a two-step reaction sequence as we have previously reported.[i] Shortly, the first step consisted in the amidation of isomeric phenylenediamines (i.e. *ortho*-phenylenediamine, *meta*-phenylenediamine and *para*-phenylenediamine) with 4-(chloromethyl)benzoyl chloride in the presence of Et_3N in CH_2Cl_2 to afford the corresponding bis-benzamides in good yields (87–96%) upon recrystallization. Their subsequent step-growth copolymerization with DABCO under equimolar conditions in DMF at 80 ºC yielded the desired polycations (i.e. 1,2-, 1,3- and 1,4-ionenes, respectively) within 2–3 days in good yields (1,2-ionene = 98%; 1,3-ionene = 69%; 1,4-ionene = 90%) after a simple filtration, washing and drying protocol. The polymers displayed same spectroscopic data to those previously reported.[1] In order to achieve adequate solubility and mobility of the polymers for GPC/SEC measurements, counteranion exchange of chloride by bis(trifluoromethanesulfonyl)amide (TFSA) anions was carried out using LiTFSA in hot water. SEC data were obtained using a YL GPC instrument equipped with a refractive index detector (temperature of column oven = 50–60 ºC; eluent = DMF including 30 mM of LiTFSA; flow rate = 0.5 mL min^{-1}). Solutions of the samples were filtered through 0.2 μm filters before injection into the 10 μm columns. Molecular weights of ionenes were calibrated using poly(methyl methacrylate) standards. Low degree of polymerizations and high dispersity values ($Đ = M_w/M_n$) are typical for these polymers and expected from step-growth polymerizations: 1,2-ionene·TFSA: $M_w = 8.1 \times 10^3$ Da; $M_n = 3.9 \times 10^3$ Da; $Đ_M = M_w/M_n = 2.1$; $n = 7$; 1,3-ionene·TFSA: $M_w = 1.2 \times 10^4$ Da; $M_n = 5.0 \times 10^3$ Da; $Đ_M = 2.4$; $n = 7$; 1,4-ionene·TFSA: $M_w = 1.7 \times 10^4$ Da; $M_n = 5.9 \times 10^3$ Da; $Đ_M = 2.9$; $n = 10$.[ii]

2. Additional Figures and Tables

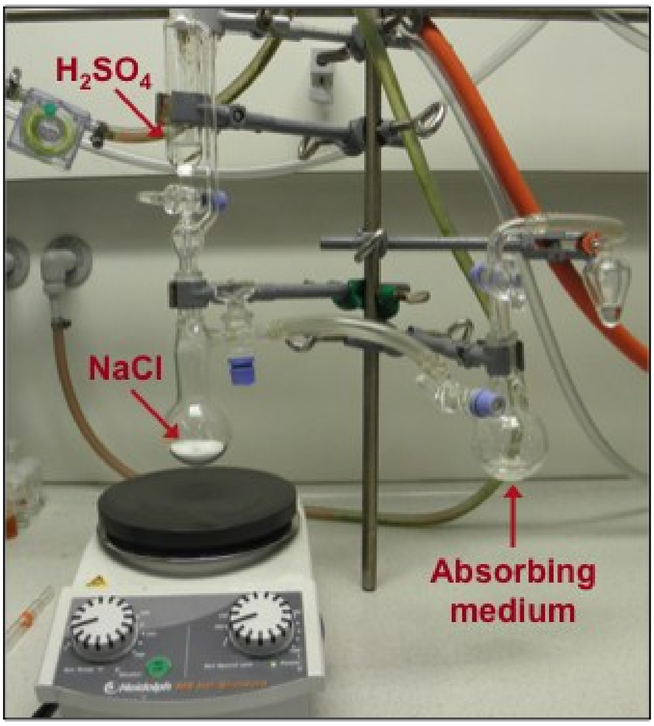

Figure S1. Experimental setup for the determination of HCl absorption. Solid **1** (500 mg) absorbed 203 mg of HCl gas in 1.5 h (4.68 g of NaCl and 4.3 mL of H_2SO_4 were used to generate HCl gas).

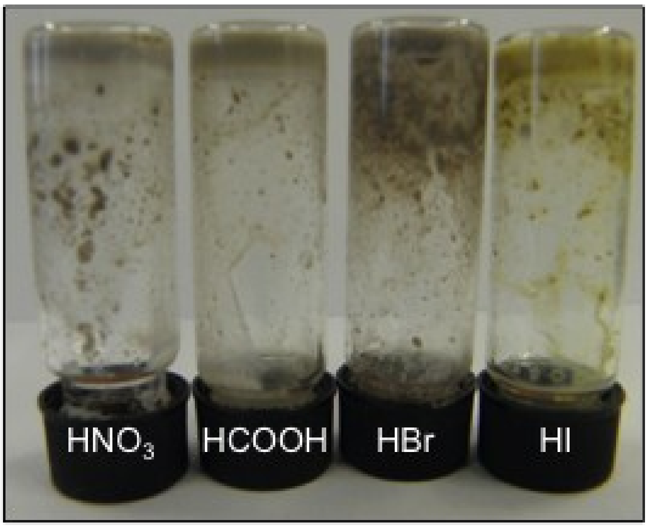

Figure S2. Appearance of the inhomogeneous gels and undissolved solid material obtained with ionene **2** (*meta*-topomer) in different acidic solutions.

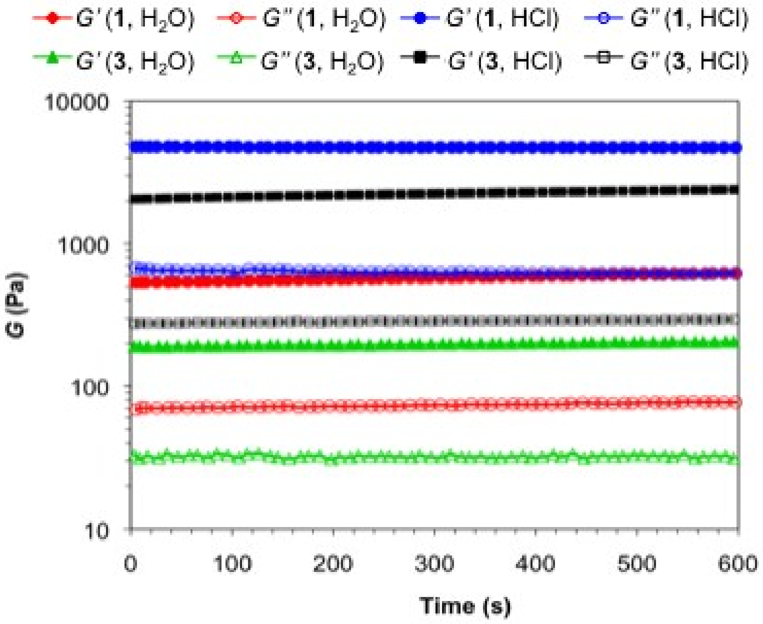

Figure S3. DTS rheological experiments of the gels prepared from **1** and **3** in water and 0.1 M HCl solution at their CGC in water as indicated in Table 1 (25 g L^{-1} and 48 g L^{-1}, respectively). For comparison, the storage modulus of agar is 43.75 kPa at a concentration of 20 g L^{-1}.

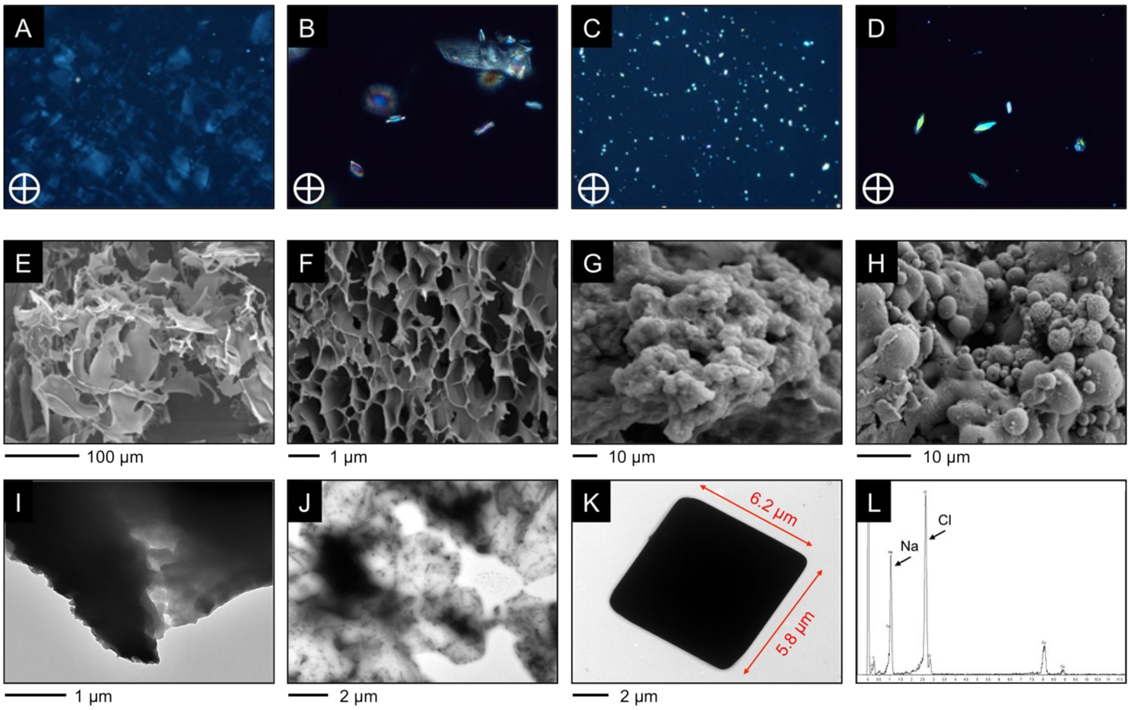

Figure S4. Optical and morphological features of hydrogels prepared from ionenes **1** and **3** at their CGC in water as indicated in Table 1. A, B) Optical images under crossed nicols of the gel film made from **1** in water. Magnification: A = 10×; B = 50×. C, D) Optical images under crossed nicols of the gel film made from **1** in 0.1 M HCl. Magnification: C = 10×; D = 50×. Note: Apparent higher birefringence density for gel-materials in acidic environment suggests the formation of more extended networks as compared to pure hydrogels, which is in agreement with their higher mechanical and thermal resistance. E) FESEM image of the xerogel derived from the gel made from **1** in water. F) FESEM image of the xerogel derived from the gel made from **3** in water. G) FESEM image of the xerogel derived from the gel made from **1** in 0.1 M HCl. H) FESEM image of the xerogel derived from the gel made from **3** in 0.1 M HCl. I) TEM image of the gel made from **1** in water. J) TEM image of the xerogel derived from **1** in 0.1 M HCl. K-L) TEM image and elemental analysis profile, respectively, of cubic structures (average edge lengths of ca. 5−15 µm) of NaCl obtained from compound **1** (25 g L^{-1}) in 0.1 M HCl solution. Such NaCl crystals were presumably formed during the preparation process of the gels/xerogels or during an aging process involving traces of Na$^+$ cations still present in the used purified water.

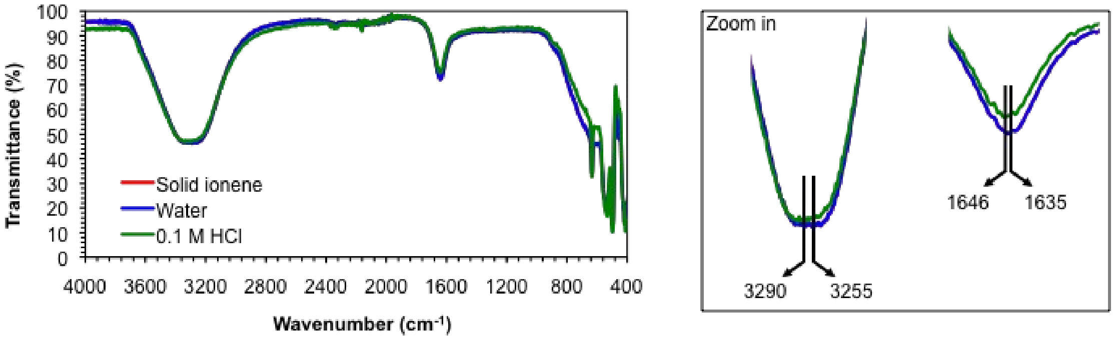

Figure S5. *Left*: Comparative FTIR spectra of hydrogels derived from compound **1** (25 g L^{-1}) in pure water, in 0.1 M HCl and in solid state. *Right*: Zoom in of given areas (blue and red lines are overlapped).

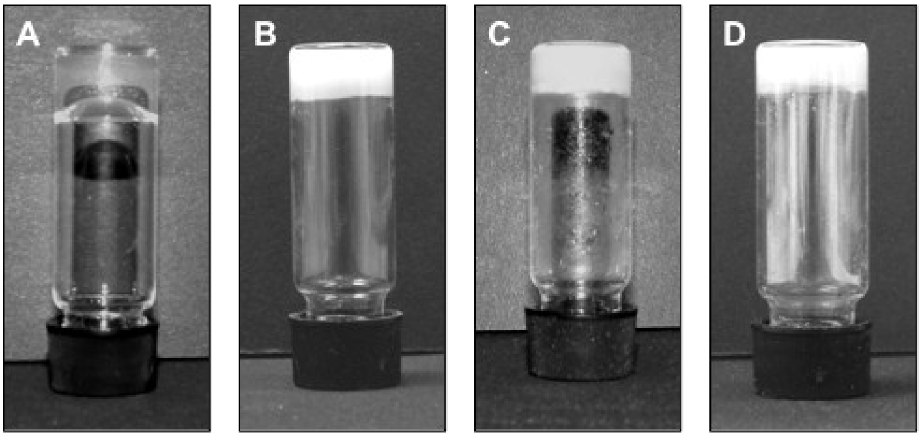

Figure S6. Digital photographs of upside-down vials containing gels derived from compounds A) **1** (25 g L^{-1}) in water, B) **1** (25 g L^{-1}) in 0.1 M HCl, C) **3** (48 g L^{-1}) in water, D) **3** (48 g L^{-1}) in 0.1 M HCl.

Table S1. Effect of the concentration of HCl on the gelation kinetics, T_{gel} and optical appearance of the gels made from ionenes **1** and **3** at their CGC in water as indicated in Table 1.[a]

Concentration HCl (M)	**Gelation time (min)**		**T_{gel} (°C)**		**Optical appearance**	
	1	**3**	**1**	**3**	**1**	**3**
0.0	1080 ± 60	2640 ± 240	56 ± 1	49 ± 1	TG	OG
0.1	20 ± 2	50 ± 5	60 ± 2	63 ± 1	OG	OG
0.25	20 ± 5	65 ± 5	59 ± 1	56 ± 2	OG	OG
0.5	40 ± 5	180 ± 15	51 ± 1	43 ± 2	OG	OG
1.0	140 ± 20	S	42 ± 2	S	WG	S
2.0	S	S	S	S	S	S

[a] Experimental errors were determined from at least two randomized measurements. Abbreviations: S = solution; TG = transparent gel; OG = opaque gel; WG = weak gel (i.e. exhibits gravitational flow after inverting a test tube within 30 min).

Table S2. Elemental analysis of the cubic structures of NaCl obtained from compound **1** (25 g L^{-1}) in 0.1 M HCl solution (see Figure S4).

Element	**Peak Area**	**Area Sigma**	**f factor**	**Abs Corrn.**	**Weight %**	**Weight% Sigma**	**Atomic %**
Na K	2378	99	1.237	1.000	36.27	1.13	46.74
Cl K	5364	140	0.964	1.000	63.73	1.13	53.26
Totals					100.00		

3. Theoretical studies

Simulated models. Simplified molecular systems for **1**, **2** and **3** hydrogels were constructed considering six polymer chains with six repeat units each one, which were initially separated by ~9Å to facilitate the formation of specific interactions. A chloride counterion was added next to each charged group (*i.e.* two positive charges per repeat unit), which represented a total of 72 counterions per molecular system. Each molecular system (*i.e.* the two polymer chains and the corresponding counterions) was placed in the centre of an orthorhombic box filled with water molecules that were previously equilibrated at 1 atm and 298 K. Those solvent molecules overlapping either a polymer atom or a chloride ion were removed. After this, 1000 randomly chosen water molecules were replaced by 1000 $H_3O^+{\cdot}Cl^-$ ion pairs. The whole systems were re-equilibrated using the following four-step protocol: (1) 8000 steps of energy minimization using the Newton Raphson method but keeping fixed the polymer chains; (2) 1 ns NVT MD at 500 K; (3) slow reduction of the temperature (10 ps/K) from 500 to 298 K using NVT MD; and (4) 0.5 ns of NPT MD. The dimensions of the simulation box, the final number of water molecules contained in the simulation box and the total number of explicit particles considered in the simulation for each molecular model are provided in Table S3.

Table S3. Details of molecular models used to simulate **4**, **5** and **6** hydrogels. All models involved 2 polymer chains with 6 repeat units and 24 chloride counterions.

Molecular system	Simulation box (Å^3)	Number of water molecules	Total number of explicit particles
1	205.6 × 157.6 × 138.3	144724	441344
2	168.0 × 199.0 × 149.0	143075	430307
3	136.5 × 194.2 × 175.0	149739	456623

Force Field details. All parameters were extrapolated from AMBER03 libraries[iii] with exception of those used to describe the H_3O^+ molecules, which were extracted from Baaden *et al.*,[iv] and the partial charges of each hydrogel repeat unit, which were taken from our previous work.[1] Water molecules were represented by the TIP3 model.[v] Van der Waals interactions were computed using an atom pair cut-off distance of 14.0 Å. In order to avoid discontinuities in the potential energy function, non-bonding energy terms were forced to slowly converge to zero, by applying a smoothing factor from a distance of 12.0 Å. Electrostatic interactions were extensively computed by means of Ewald summations. The real space term was defined by the van der Waals cutoff, while the reciprocal space was computed by interpolation into an infinite grid of points (particle mesh Ewald) with maximum space grid points being 1.0 Å.[vi] Bond lengths were constrained using the *SHAKE* algorithm[vii] with a numerical integration step of 2 fs.

Computational details. All simulations were performed using NAMD 2.7 program.[viii] The structures equilibrated after incorporate the $H_3O^+{\cdot}Cl^-$ ion pairs were the starting point of 45 ns of NPT MD simulations, in which all atoms of the system were allowed to be mobile. For these productions runs, the pressure control was performed by means of the Nose–Hoover[ix] piston combined with the piston fluctuation control implemented for Langevin Dynamics[x] for the temperature control. Pressure was kept at 1 atm, the oscillation period was set at 0.2 ps while the decay time was set at 0.06 ps. The piston temperature was set at the same value as the thermostat control, 298K, which used a damping coefficient of 1 ps^{-1}. Analyses were carried out considering the last 40 ns of MD production time.

4. References

---

i. J. Bachl, D. Zanuy, D. E. López-Pérez, G. Revilla-López, C. Cativiela, C. Alemán, and D. D. Díaz, *Adv. Funct. Mater.*, 2014, **24**, 4893–4904.

ii. J. Mayr, J. Bachl, J. Schlossmann and D. D. Díaz, *Int. J. Mol. Sci.*, 2017, **18**, 303.

iii. Y. Duan, C. Wu, S. Chowdhury, M. C. Lee, G. Xiong, W. Zhang, R. Yang, P. Cieplak, R. Luo, T. Lee, J. Caldwell, J. Wang and P. Kollman, P. *J. Comput. Chem.*, 2003, **24**, 1999–2012.

iv. M. Baaden, M. Burgard and G. Wipff, *J. Phys. Chem. B*, 2001, **105**, 11131–11141.

v. W. L. Jorgensen, J. Chandrasekhar, J. D. Madura, R. W. Impey and M. L. Klein, *J. Chem. Phys.,* 1983, **79**, 926–935.

vi. A. Toukmaji, C. Sagui, J. Board and T. Darden, *J. Chem. Phys.*, 2000, **113***,* 10913–10927.

vii. J. P. Ryckaert, G. Ciccotti and H. J. C. Berendsen, *J. Comput. Phys.*, 1977, **23**, 327–341.

viii. J. C. Phillips, R. Braun, W. Wang, J. Gumbart, E. Tajkhorshid, E. Villa, C. Chipot, R. D. Skeel, L. Kale and K. Schulten, *J. Comput. Chem.*, 2005, **26**, 1781–1802.

ix. G. J. Martyna, D. L. Tobia and M. L. Klein, *J. Chem. Phys.,* 1994, **101**, 4177–4189.

x. S. E. Feller, Y. Zhang, R. W. Pastor and B. R. Brooks, *J. Chem. Phys.*, 1995, **103**, 4613–4622.